PHYSICAL REVIEW B, VOLUME 63, 081307(R)

Femtosecond measurement of electron capture and intersubband relaxation in self-organized InAs quantum wires on $In_{1-x}Al_xAs/InP$

E. Péronne,[1] T. Polack,[1] J. F. Lampin,[1,*] F. Fossard,[2] F. Julien,[2] J. Brault,[3] M. Gendry,[3] O. Marty,[4] and A. Alexandrou[1]
[1]*Laboratoire d'Optique Appliquée Ecole Polytechnique-Ecole Nationale Supérieure de Techniques Avancées UMR CNRS 7639, Centre de l'Yvette, F-91761 Palaiseau Cedex, France*
[2]*Institut d'Electronique Fondamentale, Université Paris-Sud UMR CNRS 8622, F-91405 Orsay, France*
[3]*Laboratoire d'Electronique-LEOM, Ecole Centrale de Lyon UMR CNRS 5512, F-69131 Ecully, France*
[4]*Laboratoire d'Electronique-LENAC, Université Lyon 1, F-69622 Villeurbanne Cedex*
(Received 27 October 2000; published 7 February 2001)

We have investigated the *electron* dynamics in high-density InAs self-organized quantum wires on $In_{1-x}Al_xAs/InP(001)$ using pump-probe transmission with a midinfrared probe tuned to an intersubband transition in the conduction band. At low carrier densities, we have measured an effective capture time from the barrier to the first electron subband of 3 ps, longer than in quantum wells, and an intersubband scattering time from the second to the first subband of 0.4 ± 0.1 ps. We attribute both processes to the interaction with LO phonons. For carrier densities above 3×10^5 cm^{-1}, Auger processes lead to larger capture rates.

DOI: 10.1103/PhysRevB.63.081307 PACS number(s): 78.47.+p, 73.21.Hb, 78.30.Fs, 78.67.Lt

The electronic and optical properties of one-dimensional (1D) semiconductors, quantum wires (QWR), are fundamentally different from the properties of two- and three-dimensional semiconductors. The confinement in two dimensions results in a 1D subband structure with a strongly modified density of states showing a $1/\sqrt{E}$ singularity at each subband edge. This sharpening of the density of states was predicted to hinder energy relaxation because energy and wave-vector conservation in phonon scattering[1] as well as in carrier-carrier scattering processes[2] are more difficult to satisfy simultaneously. The modified density of states is also responsible for a number of interesting properties from the viewpoint of applications. The dipole moment associated with the intersubband transitions can be oriented perpendicular to the growth axis thus allowing the absorption of infrared radiation at normal incidence, a very promising property for midinfrared photodetector applications.

Previous studies on carrier capture and relaxation in quantum wires[3–10] have used either time-resolved photoluminescence or interband differential transmission (DT) experiments and as a consequence are sensitive to the combined electron and hole dynamics. The most direct way to probe the relaxation of only one type of carriers is to use infrared pulses tuned to an intersubband transition. Although midinfrared pulses have been applied to the electron relaxation dynamics in quantum wells,[11,12] the advantages associated with their use have hardly been exploited in the case of quantum dots[13] and wires. Furthermore, all previous studies were carried out on structures with a low lateral confinement potential (V-groove, lateral band-gap modulation structures) inducing an intersubband spacing less than the longitudinal optical (LO) phonon energy. Thus, no information is available on intersubband relaxation in quantum wires due to the LO-phonon scattering mechanism. Another consequence of the low lateral confinement is that the intersubband transitions lie in the far infrared. Therefore, the potential of quantum wires for the detection of midinfrared radiation has not been exploited up to now.

In this work, we have investigated the *electron* dynamics in a type of quantum wires (InAs on $In_{1-x}Al_xAs/InP$) featuring a high wire density[14,15] and a strong confinement potential. These properties combined with the small electron mass of InAs give rise to midinfrared intersubband transitions with giant oscillator strengths.[15,16] The originality of our measurements lies in the use of a femtosecond visible pump–infrared probe configuration: The midinfrared probe tuned to an intersubband transition allows one to isolate the electron dynamics. We report on the capture dynamics as a function of carrier density and on intersubband relaxation for a subband spacing larger than the LO-phonon energy.

The quantum wires are grown by solid-source molecular-beam epitaxy on an InP(001) substrate followed by a lattice-matched 0.4-μm thick $In_{0.52}Al_{0.48}As$ ($In_{1-x}Al_xAs$) buffer layer. The sample consists of ten planes of 0.9 nm [3 monolayers (ML)] of InAs separated by 50 nm spacer layers of $In_{1-x}Al_xAs$ and capped by 300 nm of $In_{1-x}Al_xAs$. Because of the moderate lattice mismatch (3%) between InAs and InAlAs and due to the anisotropic surface morphology of as-grown $In_{1-x}Al_xAs$, 3 ML of InAs grown on $In_{1-x}Al_xAs$ (a thickness just above the 2D/3D growth mode transition observed at 2.5 ML) without growth interruption produce self-organized wires rather than dots.[14,15]

Figures 1(a) and 1(b) show typical atomic force (AFM) and cross-sectional transmission electron microscopy (TEM) images, respectively, of samples grown in the same conditions as the one studied in this work. The AFM image shows InAs wires along the $[1\bar{1}0]$ direction with a mean length of 150 nm and a density of 3×10^5 cm^{-1}. A typical cross section of the InAs wires, according to the TEM data, is trapezoidal, 3.3 nm high, with top and base mean width of 5.5 and 22.5 nm, respectively. The wetting layer thickness lies between 0.6 and 0.9 nm. The photoluminescence spectra at 300 and 77 K [Fig. 1(c)] are centered at 845 and 960 meV with a full width at half maximum (FWHM) of 125 and 140 meV, respectively, due to the size inhomogeneities of the quantum wires.

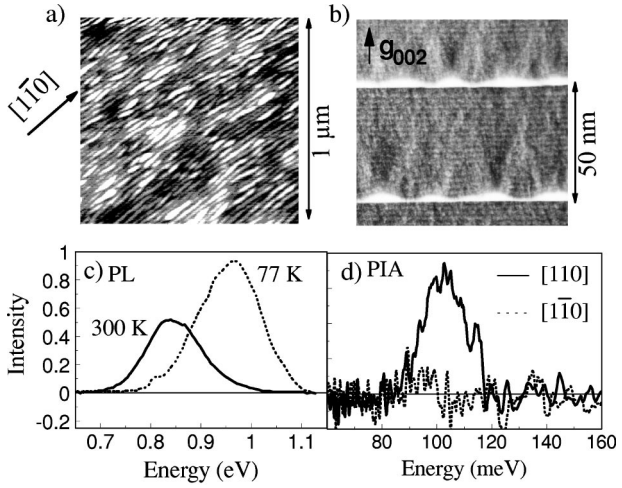

FIG. 1. (a) Atomic-force microscopy image of an uncapped InAs QWR plane. (b) Cross-sectional transmission-electron microscopy image of two QWR planes in InAlAs spacers. (c) Photoluminescence spectrum at 77 K (dashed line) and 300 K (solid line) and (d) photoinduced midinfrared absorption spectrum at 300 K of the 10-plane sample studied in this work.

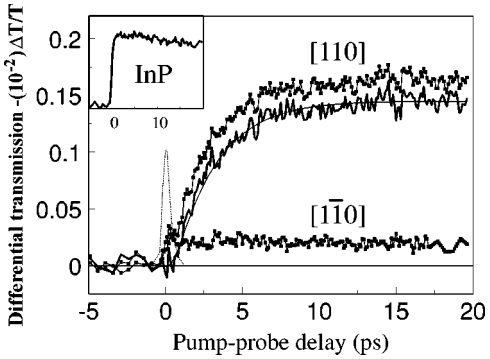

FIG. 2. Differential transmission of the QWR sample for probe polarizations along [1$\bar{1}$0] and [110] (squares). The experimental curve without symbols was obtained by subtracting the [1$\bar{1}$0]-polarized signal from the [110]-one and the solid line is a fit using a three-level rate equation model with $\tau_{c2}=2.8$ ps and $\tau_r=0.3$ ps (see text). The inset shows the DT signal of an InP substrate and the dotted line corresponds to its derivative reflecting the time resolution of the experiment with a maximum at zero pump-probe delay time.

The room-temperature photoinduced absorption (PIA) spectra excited by a cw Ar-ion laser [Fig. 1(d)] show a strong midinfrared absorption centered at 96 meV with a FWHM of 14 meV mainly due to wire size inhomogeneities. It is polarized in the layer plane perpendicularly to the quantum wires as a consequence of the lateral confinement. Experiments performed on *n*-doped samples show the same midinfrared absorption peak whereas it is absent in *p*-doped samples.[16] A record absorption of 26% at 77 K was obtained for only 10 planes doped with 1×10^{12} cm^{-2}.[15] Photoconductivity measurements in *n*-doped samples confirmed the presence of this midinfrared absorption peak.[17] We therefore ascribe this absorption to an *electronic* intersubband transition and, in particular, given the QWR dimensions (see below), to the transition between the ground and the first excited electron level. Using a crude model of a square potential along [110] (x) and [001] (z) and assuming separable variables, we can fit the interband and intersubband energies obtained from the photoluminescence and photoinduced absorption spectra for a well size of 2.92 and 17.8 nm along z and x, respectively.[18] These well size values are in good agreement with the wire cross-section dimensions obtained from the TEM data [Fig. 1(b)]. According to this calculation, there are two confined electronic levels arising from the confinement in the lateral direction (labeled $|1,1\rangle$ and $|1,2\rangle$ where the first and second number stand for the confined level number in the z and x direction, respectively), but, given the crudeness of the model, we cannot exclude the presence of a third level.

We performed DT experiments at room temperature in a femtosecond visible pump–infrared probe configuration. The midinfrared probe is obtained by difference frequency mixing between the signal and idler of an 800-nm pumped 200-kHz optical parametric amplifier.[19] Part of the 800-nm beam was used as a pump to create electron-hole pairs in the barrier, while the midinfrared probe was tuned to the intersubband transition between the first and second confined electron levels (13 μm). Therefore, these experiments are exclusively sensitive to the electron dynamics. Figure 2 shows typical DT signals for an injected carrier density of 7×10^4 cm^{-1}. The carrier density is estimated from the excitation density and the absorption of $In_{1-x}Al_xAs$ assuming that all the carriers excited in the barrier are trapped in the wires. The signals obtained for a [110]- and a [1$\bar{1}$0]-polarized probe both present a fast rising component. Only the [110]-polarized one shows a second slower rising component. Since the fast rising component is observed also in an InP substrate for both polarizations (see inset of Fig. 2), we attribute the [1$\bar{1}$0]-polarized signal to the instantaneous polarization-independent free-carrier absorption in the bulk part of the sample (capping layer, barriers, buffer, and substrate) whereas the slower rising component of the [110]-polarized DT is ascribed to the QWR absorption.

In order to extract the QWR absorption, the [1$\bar{1}$0]-polarized DT is subtracted from the [110]-polarized one. This yields the experimental curve without squares in Fig. 2. The differential signal due to the QWR absorption obtained in this way is proportional to the population difference between the two confined levels involved in the intersubband absorption. Thus, the rise time of the signal reflects the buildup of the population in the first subband. A monoexponential fit of the signal (not shown) gives a characteristic time of 3 ps which corresponds to the total time necessary for an electron to relax from the barrier down to the ground state. This time will be called the effective capture time in the following. For a probe wavelength of 10.5 μm, an effective capture time of 6 ps is measured which means that capture times are shorter in broader wires. This behavior may be due to the appearance of a third confined subband for broader wires.[20]

In general, the measured capture times are strongly dependent on the particular sample structure[5,6,9] and often in-

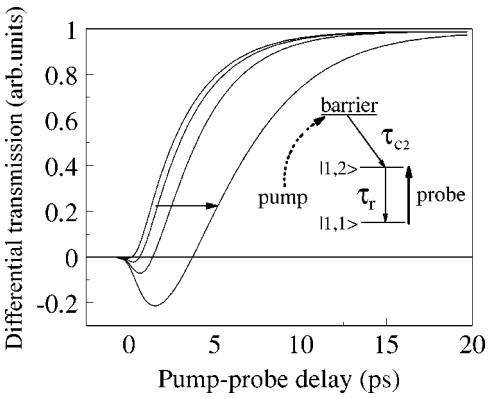

FIG. 3. Quantum-wire differential transmission signals $-\Delta T/T$ calculated with a three-level rate equation model shown in the diagram for a capture time $\tau_{c2}=2.8$ ps and for intersubband relaxation times from left to right: $\tau_r=0.3$, 0.5, 1, 3 ps. The capture time τ_{c1} is considered infinitely long.

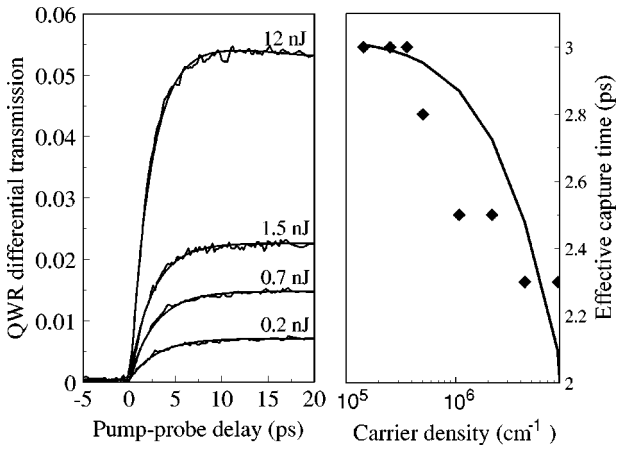

FIG. 4. Left: Differential transmission signals $-\Delta T/T$ obtained by subtracting the $[1\bar{1}0]$-polarized signals from the [110]-ones for different pump-pulse energies. The fits are monoexponentials with characteristic times of 3, 2.8, 2.5, and 2.3 ps, respectively. Right: Effective capture times obtained from the exponential fits as a function of carrier density n (diamonds) and $(A+Bn)^{-1}$ fit of the capture rate (solid line).

clude the transport processes. Experiments in InGaAs/InP quantum wells have shown that quantum capture dominates for barriers up to 50 nm.[21] In our case, due to the high density of quantum wires, and because experiments performed on samples with 15-nm thick spacer layers have shown similar capture times as those with 50-nm thick spacers, we can neglect contributions from transport processes to the capture time. Therefore, this capture time corresponds to a local or quantum capture time as defined previously in quantum wells.[21,22]

The capture times measured in our QWR system are longer than those found in quantum wells (0.3–1.8 ps),[22,21] most probably due to the reduced density of final states available for the capture process. Since the capture time was shown to oscillate in quantum wells[22] and predicted to oscillate in quantum wires[20] as a function of the energy of the last confined level with respect to the barrier, an accurate comparison between our results in quantum wires and previous results in quantum wells is only possible if the energy of the last confined level is known precisely. This, however, requires a full two-dimensional calculation of the energy levels including strain, piezoelectric field and composition distributions, which is not available at this time.

The DT due to the quantum-wire intersubband absorption shows another interesting feature around zero pump-probe delay (see Fig. 2).[23] The QWR absorption starts only a few hundred femtoseconds after the injection of carriers into the barrier. This means that the population difference takes some time to become noticeably positive, allowing us to extract an intersubband relaxation time (τ_r) as illustrated in Fig. 3. A simple three-level rate equation model taking into account the temporal resolution of our pump-probe experiment was used to calculate the population difference between the ground and the excited state for a set of τ_r, the capture time to the excited state τ_{c2} being kept constant. When τ_r is increased by a few hundred femtoseconds, the rise of the signal is shifted by about the same amount. This shift of the signal rise to positive delay times is clearly visible in Fig. 2. For longer τ_r, a negative signal appears reflecting a population inversion between the two subbands. Such a negative signal is not observed in the experiment which means that the intersubband relaxation time is short. We fit the experimental QWR DT of Fig. 2 using the three-level rate equation model in two limiting cases. In the first case, we neglect the direct capture to the ground state, τ_{c1}. Based on calculations in quantum wells[24] and dots[25] showing a much more probable capture from the barrier to excited states than to the ground state, we set, in the second limiting case, both capture times to be equal. In both cases, very good fits are obtained for $\tau_{c2}=2.8$ ps and $\tau_r=0.3$ ps (see solid line in Fig. 2) and for $\tau_{c1}=\tau_{c2}=5.6$ ps and $\tau_r=0.55$ ps (not shown). Both limiting cases correspond to a total capture time from the barrier to one of the confined wire states of 2.8 ps, while the lower and upper limits for the intersubband relaxation time are 0.3 and 0.55 ps, respectively. The intersubband relaxation time determined here is comparable to the one measured in quantum wells.[11]

Since the capture time remains constant for carrier densities up to 3.5×10^5 cm^{-1} (Fig. 4), we deduce that electron-electron scattering is negligible at such carrier densities. We thus attribute the measured capture and relaxation times to the interaction (emission and absorption) with LO phonons. The much longer intersubband relaxation times observed in V-groove wires[3,4] are related to intersubband transitions with energies below the LO-phonon energy, i.e., when LO-phonon emission is not possible. Using Fermi's golden rule we calculated an electron-phonon intersubband scattering time of 0.75 ps. Bulk LO phonons were used as in Ref. 1, since they were shown to describe the scattering process satisfactorily.[2] Given the inaccuracy of the calculated wave functions, this scattering time compares well with the experimentally determined value of 0.4 ± 0.1 ps. Defects at or near the QWR interfaces may also contribute to the electron intersubband scattering.

We also performed experiments with a pump-pulse energy varying from 0.1 to 12 nJ focused down to 100 μm.

The difference of the pump-probe signals in the two probe polarizations is depicted in Fig. 4(a) together with monoexponential fits for the rise time giving the effective capture times. For the highest pump-pulse energy a second exponential (with time constant 370 ps) had to be used in order to describe the slow decay time observed. This decay time is probably due to electron-hole recombination. It should be noted, however, that its existence does not modify the extracted effective capture time. We have not attempted to extract the evolution of the intersubband relaxation time as a function of carrier density because its value cannot be determined with sufficient precision.

Above 0.5 nJ, the rise time starts decreasing with pump intensity to reach 2.3 ps for 12 nJ. This decrease of the capture time at high excitation densities indicates a contribution of carrier-carrier scattering processes. The signals remain exponential even at high densities, i.e., no change of the capture time is observed as a function of delay time. This indicates that the total carrier population and not only the barrier population participates in the carrier-carrier scattering processes. The effective capture time is shown in Fig. 4(b) as a function of injected carrier density together with a $\tau_c^{-1}=\Gamma=A+Bn$ fit, where A is the effective capture rate observed at low densities ($0.33\ \mathrm{ps}^{-1}$), B is the coefficient describing Auger capture (1.7×10^{-8} cm / ps), and n is the carrier density.

In conclusion, we have studied strongly confined, high-density self-organized InAs quantum wires on $In_{1-x}Al_xAs/InP$ with extremely promising optical properties and, in particular, giant midinfrared electronic intersubband absorption at normal incidence. We have been able to isolate the electron dynamics thanks to a femtosecond visible pump–infrared probe technique. We have measured electron capture times longer than in quantum wells, another feature favorable for photodetector applications, and extract an electron intersubband relaxation time of 0.4 ps comparable to that in quantum wells. By varying the pump intensity by more than two orders of magnitude, we have demonstrated the contribution of carrier-carrier scattering in the acceleration of the capture process. It would be very interesting to extend this midinfrared experimental technique to quantum-dot structures and to measure the intersubband relaxation time independently from capture in an infrared pump–infrared probe scheme.

*Present address: IEMN-Dpt.ISEN, BP 69, 59652 Villeneuve d'Ascq Cedex, France.

[1] U. Bockelmann and G. Bastard, Phys. Rev. B **42**, 8947 (1990).
[2] L. Rota, F. Rossi, P. Lugli, and E. Molinari, Phys. Rev. B **52**, 5183 (1995).
[3] M. Grundmann, J. Christen, M. Joschko, O. Stier, D. Bimberg, and E. Kapon, Semicond. Sci. Technol. **9**, 1939 (1994).
[4] A. C. Maciel, C. Kener, L. Rota, J. F. Ryan, U. Marti, D. Martin, F. Morier-Genoud, and F. K. Reinhart, Appl. Phys. Lett. **66**, 3039 (1995).
[5] J. F. Ryan, A. C. Maciel, C. Kiener, L. Rota, K. Turner, J. M. Freyland, U. Marti, D. Martin, F. Morier-Genoud, and F. K. Reinhart, Phys. Rev. B **53**, R4225 (1996).
[6] A. Chavez-Pirson, H. Ando, H. Saito, N. Kobayashi, and H. Kanbe, Appl. Phys. Lett. **69**, 218 (1996).
[7] D. H. Rich and Y. Tang, Appl. Phys. Lett. **69**, 3716 (1996).
[8] R. Kumar, A. S. Vengurlekar, A. Venu Gopal, T. Mélin, F. Laruelle, B. Etienne, and J. Shah, Phys. Rev. Lett. **81**, 2578 (1998).
[9] U. Jahn, R. Nötzel, J. Ringline, H.-P. Schönherr, H. T. Grahn, and K. H. Ploog, Phys. Rev. B **60**, 11 038 (1999).
[10] V. Emiliani, T. Guenther, C. Lienau, R. Nötzel, and K. H. Ploog, Phys. Rev. B **61**, R10 583 (2000).
[11] A. Bonvalet, J. Nagle, V. Berger, A. Migus, J.-L. Martin, and M. Joffre, Phys. Rev. Lett. **76**, 4392 (1996).
[12] S. Lutgen, R. A. Kaindl, M. Woerner, T. Elsaesser, A. Hase, H. Künzel, M. Guliar, D. Meglio, and P. Lugli, Phys. Rev. Lett. **77**, 3657 (1996).
[13] S. Sauvage, P. Boucaud, F. Glotin, R. Prazeres, J.-M. Ortega, A. Lemaitre, J.-M. Gérard, and V. Thierry-Mieg, Appl. Phys. Lett. **73**, 3818 (1998).
[14] J. Brault *et al.*, Appl. Surf. Sci. (to be published).
[15] F. Fossard *et al.*, Infrared Phys. Technol. (to be published); J. Brault, M. Gendry, G. Grenet, G. Hollinger (unpublished).
[16] A. Weber, O. Gautheir-Lafaye, F. H. Julien, J. Brault, M. Gendry, Y. Dsieres, and T. Benyattou, Appl. Phys. Lett. **74**, 413 (1999).
[17] E. Finkman, S. Maimon, V. Immer, S. E. Schacham, O. Gauthier-Lafaye, S. Herriot, F. H. Julien, J. Brault, and M. Gendry (unpublished).
[18] We used $m_e=0.027m_0$ and $m_h=0.6m_0$ for the electron and hole effective mass, respectively, $E_g=413$ meV for the gap of strained InAs at room temperature, $E_g=1415$ meV for the gap of $In_{1-x}Al_xAs$, and $V_e=630$ meV for the height of the confining potential in the conduction band.
[19] M. K. Reed and M. K. Steiner Shepard, IEEE J. Quantum Electron. **32**, 1273 (1996); B. Golubovic and M. K. Reed, Opt. Lett. **23**, 1760 (1998).
[20] N. S. Mansour, Appl. Phys. Lett. **67**, 3480 (1995).
[21] B. Deveaud, J. Shah, T. C. Damen, and W. T. Tsang, Appl. Phys. Lett. **52**, 1886 (1988).
[22] P. W. M. Blom, C. Smit, J. E. M. Haverkort, and J. H. Wolter, Phys. Rev. B **47**, 2072 (1993).
[23] The zero corresponds to the coincidence of the pump and probe maxima. It is given by the delay at the middle of the rise of the free-carrier absorption signal observed for the $[1\bar{1}0]$ probe polarization.
[24] M. Abou-Khalil, M. Goano, B. Ried, A. Champagne, and R. Maciejko, J. Appl. Phys. **81**, 6438 (1997).
[25] U. Bockelmann and T. Egeler, Phys. Rev. B **46**, 15 574 (1992).